Biogeosciences Discuss., doi:10.5194/bg-2016-529, 2016
Manuscript under review for journal Biogeosciences
Published: 19 December 2016

Glycerol dialkyl glycerol tetraether variations in the northern Chukchi Sea, Arctic Ocean, during the Holocene

Yu-Hyeon Park[1, 2], Masanobu Yamamoto[1, 3], Leonid Polyak[4] and Seung-Il Nam[5]

[1]Graduate School of Environmental Science, Hokkaido University, Kita-10, Nishi-5, Kita-ku, Sapporo 060-0810, Japan

[2]Present Address; Department of oceanography, Pusan National University, Busandaehak-ro 63beon-gil, Geumjeong-gu, Busan 46241, Republic of Korea

[3]Faculty of Environmental Earth Science, Hokkaido University, Kita-10, Nishi-5, Kita-ku, Sapporo 060-0810, Japan

[4]Byrd Polar and Climate Research Center, The Ohio State University, 43210, Columbus, USA

[5]Division of Polar Paleoenvironment, Korea Polar Research Institute, 26 Songdomiraero, Yeonsu-gu, Incheon 21990, Republic of Korea

*Corresponding Author (YHP): parkyh@pusan.ac.kr

Abstract

Glycerol dialkyl glycerol tetraethers (GDGTs) have become a useful tool in paleoclimate research in ocean environments, but their applications in the Arctic are yet to be developed. GDGTs were analyzed in three sediment cores from the northern/northeastern

Biogeosciences Discuss., doi:10.5194/bg-2016-529, 2016
Manuscript under review for journal Biogeosciences
Published: 19 December 2016

margin of the Chukchi Sea to test the applicability of GDGT proxies for reconstructing sea surface temperature and sea-ice variability in the Holocene. Interpretation was enabled by an earlier investigation of GDGT composition in surface sediments from the study area. Low GDGT concentrations and high BIT and CBT values in core sediments older than ca. 8 ka probably indicate heavy sea-ice conditions in combination with terrestrial inputs during deglaciation and incomplete sea-level rise. Higher concentrations of isoprenoid GDGTs after ca. 8 ka, consistent with an increase in total organic carbon and some other biogenic proxies, are interpreted to represent increased primary production combined with elevated sedimentation rates. These patterns were likely controlled by sea-ice conditions and variations in Pacific water inflow. Geographic heterogeneity in these processes is indicated by differences in GDGTs distribution patterns between cores across the Chukchi margin. TEX_{86} and TEX_{86}^{L} indices potentially indicative of sea surface temperatures appear to show millennial-scale variability, but the controls on these fluctuations are yet to be understood.

Keywords: GDGT, TEX_{86}, TEX_{86}^{L}, BIT, MBT', CBT, Holocene, sediment records, Arctic Ocean, Chukchi Sea

1. Introduction

The Arctic Ocean currently experiences fast environmental changes due to its high sensitivity to global warming on various time scales (Screen and Simmonds, 2010; Miller et al., 2010). In particular, the Chukchi Sea (Fig. 1) is a region of dramatic changes in sea-ice and ocean current conditions due to its proximity to the North Pacific (e.g., Shimada et al., 2006). As the observational period of these changes covers only the last 2-3 decades

(Woodgate et al., 2005 a,b; Shimada et al., 2006), reconstruction of sea-ice cover and ocean circulation on time scales beyond this period is important to comprehend the ongoing processes and future climate. A number of paleo-proxy records has been obtained recently on sediment cores recovering Holocene deposits from the Chukchi region (e.g., Belicka et al., 2002; de Vernal et al., 2005, 2013; McKay et al., 2008; Darby et al., 2009, 2012; Ortiz et al., 2009; Faux et al., 2011; Polyak et al., 2009, 2016). This data suggests that the Holocene paleoceanography in the Chukchi Sea was considerably different from other Arctic margins. For example, some of the proxies indicate that while the Arctic was overall warmer in the early Holocene owing to higher summer insolation (CAPE Project Members, 2001), the Chukchi region may have had expanded sea ice, possibly related to a diminutive inflow of warm Pacific water via the Bering Strait (e.g., de Vernal et al., 2005, 2013; Polyak et al., 2016). There is also evidence that the Pacific inflow intensified and peaked in the middle Holocene (Ortiz et al., 2009; Polyak et al., 2016; Yamamoto et al., 2016). In addition to these long-term changes, higher frequency variabilities have also been identified in records with enhanced resolution (Polyak et al., 2016; Yamamoto et al., 2016).

These results pose numerous questions to the responses of the Chukchi Sea current system, sea ice, and biota to climatic changes, which can be addressed by more detailed and multifaceted proxy studies. Biomarker research, including glycerol dialkyl glycerol tetraethers (GDGTs), has a potential to augment paleoclimatic data as an independent proxy approach to paleoproductivity and hydrographic environments. We have analyzed GDGTs in three sediment cores from the northern/northeastern Chukchi Sea to evaluate changes in their abundance and composition during the Holocene (last ~10 ka) in the context of regional hydrographic and sea-ice environments. Some of the basic GDGT data on two of the studied

Biogeosciences Discuss., doi:10.5194/bg-2016-529, 2016
Manuscript under review for journal Biogeosciences
Published: 19 December 2016

cores have been used by Polyak et al. (2016) to corroborate biomarker-based sea-ice reconstructions, while regional distribution of GDGTs in surficial sediments has been reported in Park et al. (2014). In this paper we provide a comprehensive investigation of the GDGT distribution in the Holocene sediments under study. We also evaluate the applicability of GDGTs for paleoclimatic reconstructions in the Arctic seas by comparing them to other proxies in cores under study and data from other marine sites in the Chukchi-Alaskan region.

2. Material and methods

2.1 GDGT proxies

Glycerol dialkyl glycerol tetraethers (GDGTs) are increasingly used as proxies to trace environmental changes such as contribution of soil organic matter, sea surface temperature (SST), air temperature, and soil pH in the source areas (e.g., Sinninghe Damsté et al., 2000; Schouten et al., 2002; Hopmans et al., 2004; Weijers et al., 2007), but their application to Arctic marine sediments has been limited. Park et al. (2014) discussed the production, advection, and preservation of both isoprenoid and branched GDGTs as key processes determining the distribution of GDGTs and derived indices in surface sediments of the Chukchi Sea and adjacent areas of the Arctic Ocean (Fig. 2). In particular, this study demonstrates that GDGT composition in the Arctic Ocean north of the Chukchi margin (approximately 75°N) is strongly affected by allochtonous soil bacteria, while GDGTs on the Chukchi shelf have a higher marine component, and thus, a better potential for characterizing their sources and related paleoceanographic environments (Park et al., 2014). This knowledge can be now used for interpreting GDGT records in marine sediment cores from the Chukchi margin.

In this study, in addition to measured isoprenoid and branched GDGT, we empolyed TEX_{86} (TetraEther indeX of tetraethers consisting of 86 carbon atoms), MI (methane index), MBT' and CBT indices (methylation index and cyclization ratio of branched tetraethers), and BIT (Branched and isoprenoid tetraether). TEX_{86} used to reconstruct sea surface temperature (Schouten et al., 2002; Kim et al., 2010) is based on an initial global core-top dataset (Schouten et al., 2002), whereas, $TEX_{86}{}^{L}$ is based on an expanded dataset including polar waters (Kim et al., 2010). MI indicate a degree of anaerobic oxidation by Euryarchaeota (Zhang et al., 2011). High MI (> 0.4), representing high contribution of Euryarchaeota, is associated with bias of TEX_{86} values. MBT' and CBT have been proposed as proxies of soil pH and mean annual air temperature (Peterse et al., 2012; Weijers et al., 2007), and BIT as a proxy of soil organic matter contribution (Hopmans et al., 2004; Kim et al., 2006). These indices have been shown useful for identifying the sources of branched GDGT in the study region (Park et al., 2014).

2.2 Samples and age constraints

Sediment cores ARA02B 01A-GC (gravity core) and HLY0501-05TC/JPC, -06JPC and -08TC/JPC (trigger/ jumbo piston cores), hereafter referred to as 01A-GC, 05JPC, 06JPC and 08JPC, were collected from the northern to northeastern margin of the Chukchi shelf during the 2011 cruise of the RV Araon and 2005 cruise of USCG Healy (Table 1; Fig. 1). Trigger cores are used for a better representation of the uppermost soft sediments that may have been missed by respective piston cores due to overpenetration. Cores 01A-GC and 08JPC are sited on the outer shelf in water depths of 111 and 90 m, which were above the sea level at the time of the last glaciation and inundated during the postglacial transgression since about 15 ka

Biogeosciences Discuss., doi:10.5194/bg-2016-529, 2016
Manuscript under review for journal Biogeosciences
Published: 19 December 2016

(e.g., Keigwin et al., 2006). In contrast, cores 05JPC and 06JPC were raised from the continental slope at 462 m and 673 m depth, where sediment deposition was not interrupted by sea-level changes. Only a few samples from the bottom part of stratigraphically most extensive 06JPC are used in this study to augment the 05JPC record.

Various stratigraphic and sedimentological data on one or several of the cores under study have been reported in a number of papers (Barletta et al., 2008; McKay et al., 2008; Darby et al., 2009, 2012; Polyak et al., 2009, 2016; Lisé-Pronovost et al., 2009; Brachfeld et al., 2009; Faux et al., 2011; Kim et al., 2016). Sediments in cores 08JPC and 01A-GC consist predominantly of homogenous clayey silts indicative of open-marine environments, with a more sandy composition near the core bottom, possibly related to shallow-water erosion and redeposition during the shelf flooding (Darby et al., 2009). In cores 05JPC and 06JPC the homogenous, fine-grained marine unit is underlain by a more complex lithostratigraphy with laminations and coarse ice-rafted debris indicative of glaciomarine environments affected by glacial/deglacial processes (McKay et al., 2008; Lisé-Pronovost et al., 2009; Polyak et al., 2009).

In total 110, 47, 2 and 34 samples were collected for the GDGT analysis from cores 01A-GC, 05JPC, 06JPC, and 08JPC, respectively. Samples were mostly taken from the Holocene marine sediments at intervals providing a multidecadal- to multicentury-scale resolution. In addition, several samples from the lower part of cores 05JPC and 06JPC span the pre-Holocene sedimentary sequence. Samples were stored in a refrigerator since collection, subsampled and freeze-dried for further processing.

Age constraints were provided by seven, six, and ten accelerator mass spectrometry (AMS) ^{14}C ages of mollusc shells from cores 01A-GC (Kim et al., 2016), 05JPC, and 08JPC

(Darby et al., 2009), respectively (Supplementary Table S1; Fig. 3). ^{14}C ages were converted to calendar ages using the CALIB7.0 program and marine13 dataset (Reimer et al., 2013). Local reservoir corrections (ΔR) were taken as 500 years for 01A-GC and 08JPC washed by surface waters and 0 years for 05JPC washed by subsurface Atlantic waters (McNeely et al., 2006; Darby et al., 2012).

The age model was constructed by linear interpolation between the dating points, which fall within the interval of ca. 1.5–8.6 ka (Fig. 3), as well as the assumed modern age of the core tops. Ages below the dated interval were extrapolated to the bottom of cores 01A-GC and 08JPC and to the bottom of marine unit in stratigraphically longer core 05JPC. Core 05JPC was further expanded by the addition of two samples from the nearby core 06JPC. Rough age constraints for older sediments in cores 05JPC and 06JPC were estimated by correlation with cores from the adjacent western Arctic Ocean (Polyak et al., 2009), where samples from core 05JPC span the last deglaciation, and the two samples from core 06JPC possibly represent pre-LGM (> ca. 25 ka) environments. Due to inevitable inaccuracies in the age estimation beyond the dated interval, the bottom of marine sediments in the 01A-GC, 05JPC and 08JPC came out with slightly different ages between ca. 8.5–9.5 ka, so we assume that the actual age of this stratigraphic boundary is close to 9 ka. The distribution of linear sedimentation rates shows maximal values in all studied cores around 5–6 ka, with especially high rates in core 08JPC (Fig. 3). The synchroneity of this peak corroborates the validity of the difference in ΔR used for cores from different water masses (01A-GC and 08JPC vs. 05JPC).

Sedimentation rates estimated from ^{210}Pb measurements in the upper 15 cm in 05TC suggest somewhat younger ages than those derived from available ^{14}C datings (McKay et al., 2008). While comparing these two approaches require more precise chronostratigraphic constraints, in this study we used the ^{14}C-based age model because of the uncertainty with extrapolating ^{210}Pb-based age estimates related to potential variability in sedimentation rates. We note that the difference applies only to the uppermost part of the stratigraphy and does not have a considerable effect on the conclusions of this study.

2.3 GDGT analysis

Freeze-dried and homogenized sediments were extracted using accelerated solvent extractor (DIONEX ASE-200) with 11 ml of mixture of dichloromethane:methanol (6:4, v:v) at 100 °C and 1000 psi for 10 minutes (×3). The extract was concentrated by a rotary evaporation and then separated into four fractions (F1 to F4) depending on polarity of lipid by silica gel column chromatography. F4 fraction including GDGTs, treated according to procedure of Yamamoto and Polyak (2009), was analysed using HPLC/MS (high performance liquid chromatography/mass spectrometry) connected to a Bruker Daltonics micrOTOF-HS time-of-flight MS. GDGTs were separated using an Alltech Prevail Cyano column (2.1×150 mm, 3 μm) at 30 °C in HPLC and identified according to Hopmans et al. (2000) and Schouten et al. (2007). GDGTs investigated for this study are shown in the Appendix. TEX_{86} and TEX_{86}^{L} were calculated according to Schouten et al. (2002) and Kim et al. (2010), respectively, and converted to temperature using calibration suggested by Kim et al. (2010; T (°C) = 81.5 TEX_{86} – 26.6; T(°C) = 67.5 TEX_{86}^{L} + 46.9). The standard deviations (SD) of TEX_{86} and TEX_{86}^{L} derived temperatures were 0.8 °C and 1.5 °C, repectively. MI, BIT, CBT indexes were calculated according to Zhang et al. (2011), Hopmans et al. (2004) and Weijers et al. (2007), respectively. The SD of MI, BIT, CBT were averaged 0.002, 0.002,

Biogeosciences Discuss., doi:10.5194/bg-2016-529, 2016
Manuscript under review for journal Biogeosciences
Published: 19 December 2016

0.009, respectively. MBT' was calculated according to Peterse et al. (2012), and the SD was 0.006.

3. Results

Isoprenoid GDGTs detected include GDGT-0, GDGT-1, GDGT-2, GDGT-3, crenarchaeol, and crenarchaeol regioisomer (Structures are shown in the Appendix). Crenarchaeol and GDGT-0 are the most abundant isoprenoid GDGTs in the studied samples (Fig. 4). In the averaged fractional abundance of isoprenoid GDGTs, crenarchaeol in cores 01A-GC and 08JPC is most abundant during middle and late Holocene, comparable to GDGT values in surface sediment from the shelf edge of the Chukchi Sea (Fig. 4). Fractional abundances of isoprenoid GDGTs show a considerable variability at the transition from early to middle Holocene, especially in core 05JPC.

Total concentrations of isoprenoid GDGT have highest values in core 01A-GC, from 2.6 to 31.6 μg/g, and do not exceed 18.4 μg/g in cores 05JPC and 08JPC (Fig. 5). Concentrations vary between the cores but show similar, stratigraphically consistent downcore patterns, especially for cores 01A-GC and 05JPC. In the late deglacial interval to early Holocene (until ca. 9 ka) concentrations were low in all three cores, then increased markedly to ca. 7–8 ka, and reached a maximum around ca. 5–6 ka in cores 01A-GC and 05JPC. In the late Holocene, isoprenoid GDGTs had overall high but variable concentrations, with a distinct maximum around 3 ka in 08JPC. Near the core top in 01A-GC, 05JPC and 08JPC concentrations show a decrease. In the deglacial unit studied in core 05JPC, isoprenoid GDGT get relatively more abundant towards the bottom. In the yet older (possibly pre-LGM) sediment recovered in core 06JPC, the concentrations of isoprenoid GDGT were low.

Branched GDGTs detected include I, Ib, Ic, II, IIb, IIc, III, IIIb, and IIIc (Structures are shown in the Appendix). Acyclic GDGTs such as I, II and III are the most abundant in the studied sediments (Fig. 4). Whereas acyclic GDGTs are abundant in core 05JPC and 08JPC during the entire Holocene, GDGT-IIb is also abundant in core 01A-GC, especially in the middle and late Holocene, with values comparable to surface sediment from the shelf edge of the Chukchi Sea (Fig. 4). Branched GDGTs show a considerable difference in fractional abundances between middle and early Holocene, especially in core 05JPC, similar to isoprenoid GDGTs (Fig. 4). The total concentrations of branched GDGTs reach 1.3 µg/g, 1.1 µg/g, and 1.9 µg/g in cores 01A-GC, 05JPC, and 08JPC, respectively (Fig. 5). Like isoprenoid GDGTs, the branched GDGTs concentrations show a similar downcore distribution pattern. In all studied cores, concentrations were low until ca. 9 ka, and then increased to around 8 ka. The peak at ca. 5–6 ka is well expressed in cores 01A-GC and 05JPC, followed by variable concentrations with another, somewhat lower maximum at 1–2 ka. In core 08JPC maximal values were reached around 7 ka and 3 ka. An increase in branched GDGTs is also evident at the bottom of the deglacial unit in core 05JPC, whereas, low concentrations characterize the two older samples from core 06JPC (Fig. 5).

The BIT index shows highest levels of >0.5 in the deglacial unit, decreases to very low levels by ca. 7–8 ka, and stays consistently low since then in cores 01A-GC and 05JPC (Fig. 5). In core 08JPC, BIT decreases with some fluctuations from >0.3 at 9–10 ka to 0.1 by 3 ka, and then slightly increases towards the core top. In the early deglacial and older sediments in cores 05JPC/06JPC, BIT values are lower than later in deglaciation to early Holocene, but somewhat higher than in the late Holocene (Fig. 5).

The ratio of GDGT-0 to crenarchaeol (GDGT-0/cren) and the MI are overall low except for somewhat elevated values in the early Holocene until ca. 8 ka in cores 05JPC and 08JPC (Fig. 5).

The distribution of the CBT index is similar to that of the BIT (Fig. 5). Maximal CBT values characterize the early Holocene and decrease to low levels by 7–8 ka in cores 01A-GC and 05JPC. In 08JPC the Holocene CBT is somewhat higher and shows an overall decrease towards ca. 3 ka and a slight increase thereafter. In the early deglacial and older section in cores 05JPC/06JPC, CBT values are relatively elevated, but not as much as in later deglacial to early Holocene sediments.

The MBT' index also shows relatively high values in the early Holocene with a peak around 10 ka in core 05JPC and another peak around 8 ka (Fig. 5). In core 08JPC MBT' is variable with peaks at ca. 6, 7 and 8 ka. In core 01A-GC the MBT' shows less variability.

TEX_{86}-derived temperatures strongly fluctuate, ranging mostly between 5 and 15 °C with a slight general increase throughout the Holocene in cores 01A-GC and 05JPC (Fig. 5). No such trend occurs in core 08JPC. TEX_{86}^{L}-derived temperatures are overall lower by up to 10 °C than TEX_{86}-derived temperatures and show no trend in their distribution. In core 01A-GC, the amplitude of TEX_{86}^{L} fluctuations increases noticeably after ca. 6 ka.

4. Discussion

4.1. Changes in production and sources of GDGTs during the Holocene

GDGT distribution in surface sediments from the Chukchi Sea and the adjacent western Arctic Ocean and northern Bering Sea shows abundant isoprenoid GDGTs on the outer shelf and slope of the Chukchi Sea and the upper slope of the Bering Sea (Fig.2; Park et al., 2014).

The higher abundances are attributed to a combination of higher production of marine Archaea (Thaumarchaeota) at the shelf edge, redeposition of GDGT-carrying fine sediment particles from the shelf, and better preservation of GDGTs at sites with higher sedimentation rates.

The fast increase in isoprenoid GDGTs is observed in all three studied cores at the bottom of marine sedimentary unit, from ca. 9 to 8 ka (Fig. 6). This change is consistent with an increase in total organic carbon and some other biogenic proxies, such as silica, in these and nearby cores (Darby et al., 2001; Lundeen, 2005; McKay et al., 2008; Currie, 2009, and unpublished data for 01A-GC). This correspondence suggests that the increase in isoprenoid GDGT concentrations was driven by increasing bioproduction with the establishment of marine environments in the Chukchi Sea after the end of deglaciation and opening of sufficient inflow through the Bering Strait.

Further changes in isoprenoid GDGT concentrations are more complex. The peak values around 5-6 ka in cores 01A-GC and 05JPC correspond to maximal sedimentation rates (Fig. 5) suggesting that preservation may have been a factor. However, no isoprenoid GDGT peak occurs in core 08JPC at this time despite a well expressed sedimentation rate maximum. This discrepancy indicates that isoprenoid GDGT concentrations were primarily controlled by factors other than preservation, like primary production, which could have varied spatially due to differing sea- ice conditions. A comparison with the distribution of sea-ice related biomarker IP_{25} shows that concentrations of isoprenoid GDGTs in both cores increased after the decline of IP_{25} values peaking at ca. 5–6 ka in 5JPC and ca. 3 ka in 8JPC (Fig. 5; Polyak et al., 2016). This offset of isoprenoid GDGT peaks relative to IP_{25} is consistent with the inferred negative effect of sea ice on local GDGT production (Park et al., 2014). Another possibility is that the GDGT peak in cores 01A-GC and 05JPC was related to an increase in the Bering Strait inflow in the middle Holocene (Ortiz et al., 2009; Polyak et al., 2016), which may have had different effects in the northern and eastern parts of the Chukchi Sea washed by different branches of the Bering Strait inflow (Fig. 1). In the pre-Holocene section, a relative increase in isoprenoid GDGTs near the bottom of deglacial sediments in core 05JPC (Fig. 5) might represent a post-LGM warming and resultant sea ice retreat and enhanced primary production, such as during the Bølling/Allerød period, but the age control is insufficient to constrain this interval.

Branched GDGTs in surface sediments are abundant on the Chukchi shelf and in the Yukon and Mackenzie River estuaries (Fig.2; Park et al., 2014). A concerted abundance of both branched and isoprenoid GDGTs at the Chukchi shelf edge indicates common concentration processes, such as sediment redeposition and enhanced preservation at sites with high sedimentation rates. High cyclization ratios of branched tetraethers (CBT) characterisze sediments from the Arctic Ocean north of the Chukchi margin (~75 °N), as well as the Yukon and Mackenzie River estuaries, in contrast to lower CBT in sediments from the Chukchi and Bering seas. This difference indicates two principal sources of branched GDGTs tentatively interpreted as soil bacteria and in situ marine bacteria, respectively.

High BIT and CBT vs. MBT' values peaking in the deglacial sediments and extending into lower Holocene until ca. 8 ka, as expressed especially clearly in cores 01A-GC and 05JPC (Fig. 6), are similar to these indices in surface sediments of the study region north of 75 °N (Park et al., 2014). Fig. 4 also shows similarity in fractional distribution of branched GDGTs between the early Holocene interval in the studied cores and offshore areas of Chukchi Sea. These high BIT and CBT values along with low GDGT concentrations north of

Biogeosciences Discuss., doi:10.5194/bg-2016-529, 2016
Manuscript under review for journal Biogeosciences
Published: 19 December 2016

75 °N were interpreted as a result of very low marine production and/or severe degradation under multi-year ice, and thus relatively high content of imported terrestrial GDGTs. We infer that similar conditions prevailed in the study area in the early Holocene before ca. 8 ka. This conclusion is consistent with the dinocyst-based proxy record from core 05JPC indicative of high sea-ice concentration in the early Holocene (McKay et al., 2008). Other dinocyst studies from this region also show a generally similar pattern (de Vernal et al., 2005; 2008; 2013; Farmer et al., 2011), but lack resolution or stratigraphic recovery for a comprehensive characterization of the early Holocene. In addition to the effect of high sea-ice concentration in the early Holocene, low Bering Strait inflow and elevated freshwater inputs due to incomplete sea-level rise and deglacial processes (Darby et al., 2001; Lundeen, 2005; Yamamoto et al., in review) could inhibit marine production and enhance import of terrestrial material in the northern Chukchi Sea.

BIT and CBT vs. MBT' values in the early deglacial and older sediments in cores 05JPC/06JPC show intermediate levels between the deglacial to early Holocene and middle-late Holocene data (Figs. 4–6). This suggests the possibility of either relatively high organic production (low ice concentrations) during those times or redeposition of organic material from stratigraphically older deposits. The latter may be especially applicable to 06JPC samples that show very low isoprenoid GDGT concentrations.

4.2. Variations in TEX_{86} and TEX_{86}^{L}

Based on GDGT distribution in surface sediments from the study region Park et al. (2014) concluded that TEX_{86} and TEX_{86}^{L} indices are not applicable for SST reconstructions north of roughly 73 °N. Further south in the Chukchi Sea, these indices show a more reasonable relation to SST, although still off the global core top calibration curve (Kim et al., 2010). Therefore, one must be cautious about translating TEX_{86} and TEX_{86}^{L} data into absolute SST values in the study area. Nevertheless, relative downcore changes in TEX_{86} and TEX_{86}^{L} may be indicative of SST variability, especially in full-marine environments. GDGT distribution in surficial shallow-water sediments shows that high BIT, GDGT-0/cren, and MI indices relate to high TEX_{86} and TEX_{86}^{L} values, indicating their terrestrial bias (Park et al., 2014). However, in full-marine sediments deposited in cores under study after ca. 8-9 ka, these indices are consistently low (Fig. 5), suggesting that variation in TEX_{86} and TEX_{86}^{L} here is not related to terrestrial contribution or appreciable methanotrophic euryarchaea, which can produce GDGT-1, GDGT-2 and GDGT-3.

A millennial- to multicentury-scale variability in TEX_{86}- and TEX_{86}^{L}-derived SST is well expressed in the investigated Holocene records, especially in core 01A-GC studied with the highest resolution (Fig. 5). This variability appears to increase in amplitude, along with a slight increase in TEX_{86}- and TEX_{86}^{L}-derived SST values, during the Holocene towards the core top. This variation does not resemble the record of chlorite abundance reflecting the strength of Bering Strait inflow (Ortiz et al., 2009) nor the proxy records of sea-ice cover (de Vernal et al., 2013; Polyak et al., 2016). This differing pattern suggests that neither Pacific water advection nor sea-ice cover had a major control on TEX_{86} and TEX_{86}^{L} variability in the northern Chukchi Sea. More studies are needed to understand the controls on these indices and their applicability for SST reconstructions in the Arctic.

5. Conclusions

The analysis of GDGTs in three sediment cores from the northern/northeastern Chukchi

Sea margin provides insights into GDGTs production and sources in this region of the Arctic during the Holocene. Concentrations of isoprenoid GDGTs reached high values by ca. 8 ka with the establishment of marine conditions after deglaciation and sea-level rise. Low GDGTs concentrations combined with high BIT and CBT values prior to ca. 8 ka may suggest high concentrations of sea-ice in the northern Chukchi Sea, with overall milder sea-ice conditions later in the Holocene. Higher inputs of terrestrial material were also likely during the deglaciation extending into the early Holocene. After ca. 8 ka, GDGTs distribution was variable and probably controlled by a combination of sea-ice conditions and Bering Strait inflow that affected primary production and sediment transport and deposition. Different patterns in GDGTs distribution between cores from the northern and northeastern sites may indicate spatial differences in the pathways of Pacific waters and sea-ice extent. TEX_{86} and TEX_{86}^{L} indices potentially useful for SST reconstruction show millennial-scale variability, but the controls are not well understood. More investigations using multiple proxies are needed to comprehend sea-ice, temperature, and circulation history in the Chukchi Sea, a critical region for the Arctic climate change.

Acknowledgements

We thank all of the captain, crew and scientists of RV ARAON and IB USCGC Healy for their help during the cruise of sampling. We also thank K. Ohnishi of Hokkaido University for analytical assistance. The study was supported by a grant-in-aid for Scientific Research (B) the Japan Society for the Promotion of Science, No. 25287136 (to M.Y.), Basic Research Program (PE16062) of Korea Polar Research Institute (to S.I.N), and Atmospheric See-At Technology Development Program, Grant No. KMIPA 2015-6060 (to YHP).

References

Barletta, F., St-Onge, G., Channell, J.E.T., Polyak, L., Darby, D.A., 2008. High-resolution paleomagnetic secular variation and relative paleointensity records from the western Canadian Arctic: implication for Holocene stratigraphy and geomagnetic field behaviour. Can. J. Earth Sci. 45, 1265–1281.

Belicka, L.L., Harvey, H.R., 2009. The sequestration of terrestrial organic carbon in Arctic Ocean sediments: A comparison of methods and implications for regional carbon budgets. Geochimica et Cosmochimica Acta, 73, 6231–6248.

Belicka, L.L., MacDonald, R.W., Harvey, H.R., 2002. Sources and transport of organic carbon to shelf, slope, and basin surface sediments of the Arctic Ocean. Deep-Sea Research I 49, 1463–1483.

Brachfeld, S., Barletta, F., St-Onge, G., Darby, D.A., Ortiz, J.D., 2009. Impact of diagenesis on the environmental magnetic record from a Holocene sedimentary sequence from the Chukchi–Alaskan margin, Arctic Ocean. Global Planet. Change 68, 100–114.

CAPE Project Members, 2001. Holocene paleoclimate data from the Arctic: testing models of global climate change. Quaternary Science Reviews 20, 1275–1287.

Cota, G.F., Pomeroy, L.R., Harrison, W.G., Jones, E.P., Peters, F., Sheldon, W.M., Weingartner, T.R., 1996. Nutrients, primary production and microbial heterotrophy in the southeastern Chukchi Sea: Arctic summer nutrient depletion and heterotrophy. Marine Ecology Progress Series 135, 247–258.

Curry, A.C., 2009. Biogenic tracers through the Holocene on the Alaskan shelf. MS Thesis, Old Dominion Univ., 90 p.

Darby, D.A., 2003. Sources of sediment found in sea ice from the western Arctic Ocean, new insights into processes of entrainment and drift patterns. Journal of Geophysical Research 108, 3257, doi:10.1029/2002JC001350.

Darby, D.A., Bischof, J., Cutter, G., de Vernal, A., Hillaire-Marcel, C., Dwyer, G., McManus, J., Osterman, L., Polyak, L., Poore, R., 2001. New record shows pronounced changes in Arctic Ocean circulation and climate. Eos 82, No. 49, 601, 607.

Darby, D.A., Ortiz, J.D., Grosch, C.E., Lund, S.P., 2012. 1,500-year cycle in the Arctic Oscillation identified in Holocene Arctic sea-ice drift. Nature geoscience 5, 897–900.

Darby, D.A., Ortiz, J.D., Polyak, L., Lund, S., Jakobsson, M., Woodgate, R.A., 2009. The role of currents and sea ice in both slowly deposited central Arctic and rapidly deposited Chukchi–Alaskan margin sediments. Global and Planetary Change 68, 58–72.

De Jonge, C., Stadnitskaia, A., Hopmans, E. C., Cherkashov, G., Fedotov, A., Damsté, J. S. S., 2014. In situ produced branched glycerol dialkyl glycerol tetraethers in suspended particulate matter from the Yenisei River, Eastern Siberia. Geochimica et Cosmochimica Acta 125, 476–491.

De Jonge, C., Stadnitskaia, A., Hopmans, E. C., Cherkashov, G., Fedotov, A., Streletskaya, I. D., Vasiliev, A.A., Damsté, J. S. S., 2015. Drastic changes in the distribution of branched tetraether lipids in suspended matter and sediments from the Yenisei River and Kara Sea (Siberia): Implications for the use of brGDGT-based proxies in coastal marine sediments. Geochimica et Cosmochimica Acta 165, 200–225.

de Vernal, A., Hillaire-Marcel, C., Darby, D.A., 2005. Variability of sea-ice cover in the Chukchi Sea (western Arctic Ocean) during the Holocene. Paleoceanograpy 20, PA4018.

de Vernal, A., Hillaire-Marcel, C., Rochon, A., Fréchette, B., Henry, M., Solignac, S., Bonnet, S., 2013. Dinocyst-based reconstructions of sea ice cover concentration during the Holocene in the Arctic Ocean, the northern North Atlantic Ocean and its adjacent seas. Quaternary Science Reviews 79, 111–121.

Dyke, A.S., Savelle, J.M., 2001. Holocene history of the Bering Sea bowhead whale (Balaena mysticetus) in its Beaufort Sea summer grounds off southwestern Victoria Island, western Canadian Arctic. Quaternary Research 55, 371–379.

Farmer, J.R., Cronin, T.M., de Vernal, A., Dwyer, G.S., Keigwin, L.D., Thunell, R.C., 2011. Western Arctic Ocean temperature variability during the last 8000 years. Geophysical Research Letters 38, L24602.

Faux J.F., Belicka, L.L., Harvey, H.R., 2011. Organic sources and carbon sequestration in Holocene shelf sediments from the western Arctic Ocean. Continental Shelf Research 31, 1169–1179.

Hill, V.J., Cota, G.F., 2005. Spatial patterns of primary production, in the Chukchi Sea in the spring and summer of 2002, Deep Sea Research Part II 52, 3344–3354.

Ho, S. L., Mollenhauer, G., Fietz, S., Martínez-Garcia, A., Lamy, F., Rueda, G., Schipper, K., Méheust, M., Rosell-Melé, A., Stein, R., Tiedemann, R., 2014. Appraisal of TEX_{86} and TEX_{86}^{L} thermometries in subpolar and polar regions. Geochimica et Cosmochimica Acta 131, 213–226.

Hopmans, E.C., Schouten, S., Pancost, R.D., van der Meer, M.T.J., Sinninghe Damsté, J.S., 2000. Analysis of intact tetraether lipids in archaeal cell material and sediments by high performance liquid chromatography/atmospheric pressure chemical ionization mass spectrometry. Rapid Communications in Mass Spectrometry 14, 585–589.

Biogeosciences Discuss., doi:10.5194/bg-2016-529, 2016
Manuscript under review for journal Biogeosciences
Published: 19 December 2016

Hopmans, E.C., Weijers, J.W.H., Schefuss, E., Herfort, L., Sinninghe Damsté, J.S., Schouten, S., 2004. A novel proxy for terrestrial organic matter in sediments based on branched and isoprenoid tetraether lipids. Earth and Planetary Science Letters 24, 107–116.

Huguet, C., Hopmans, E.C., Febo-Ayala, W., Thompson, D.H., Sinninghe Damsté, J.S.S., Schouten, S., 2006. An improved method to determine the absolute abundance of glycerol dibiphytanyl glycerol tetraether lipids. Organic Geochemistry 37, 1036–1041.

Keigwin, L.D., Donnelly, J.P., Cook. M.S., Driscoll, N.W., Brigham-Grette, J., 2006. Rapid sea level rise and Holocene climate in the Chukchi Sea. Geology 34, 861–864.

Kim, J. H., Crosta, X., Willmott, V., Renssen, H., Bonnin, J., Helmke, P., Schouten, S., Sinninghe Damsté, J. S., 2012. Holocene subsurface temperature variability in the eastern Antarctic continental margin. Geophysical Research Letters 39. L06705.

Kim, J.-H., van der Meer, J., Schouten, S., Helmke, P., Willmott, V., Sangiorgi, F., Koc, N., Hopmans, E.C., Sinninghe Damsté, J.S., 2010. New indices and calibrations derived from the distribution of crenarchaeal isoprenoid tetraether lipids: implications for past sea surface temperature reconstructions. Geochimica et Cosmochimica Acta 74, 4639–4654.

Kim, J. H., Schouten, S., Buscail, R., Ludwig, W., Bonnin, J., Sinninghe Damsté, J. S., & Bourrin, F., 2006. Origin and distribution of terrestrial organic matter in the NW Mediterranean (Gulf of Lions): Exploring the newly developed BIT index. Geochemistry, geophysics, geosystems, 7(11).

Kim, J. H., Schouten, S., Rodrigo-Gámiz, M., Rampen, S., Marino, G., Huguet, C., Helmke, P., Buscail, R., Hopmans, E. C., Pross, J., Sangiorgi, F., Middelburg, J. B. M., Sinninghe Damste, J. S., 2015. Influence of deep-water derived isoprenoid tetraether lipids on the paleothermometer in the Mediterranean Sea. Geochimica et Cosmochimica Acta 150, 125–141.

Kim, S.-Y., Polyak, L., Delyusina, I., Nam, S.-I., 2016. Terrestrial and aquatic palynomorphs in Holocene sediments from the Chukchi-Alaskan margin, western Arctic Ocean: implications for the history of marine circulation and climatic environments. The Holocene, in press.

Lisé-Pronovost, A., St-Onge, G., Brachfeld, S., Barletta, F., Darby, D., 2009, Paleomagnetic constraints on the Holocene stratigraphy of the Arctic Alaskan margin. Global Planet. Change 68, 85–99.

Lundeen, Z., 2005. Elemental and isotopic constraints on the Late Glacial–Holocene transgression and paleoceanography of the Chukchi Sea. MS Thesis, Univ. Massachussetts Amherst, 91 p.

McKay, J., de Vernal, A., Hillaire-Marcel, C., Not, C., Polyak, L., Darby, D., 2008. Holocene fluctuations in Arctic sea-ice cover: Dinocyst-based reconstructions for the eastern Chukchi Sea. Canadian Journal of Earth Sciences 45, 1377–1397.

McNeely R., Dyke A. S., Southon J. R., 2006. Canadian marine reservoir ages, preliminary data assessment, Open File Rept. 5049, pp. 3. Geological Survey Canada.

Miller, G.H., Alley, E.B., Brigham-Grette, J., Fitzpatrick, J.J., Polyak, L., Serreze, M.C., White, J.W.C., 2010. Arctic amplification: can the past constrain the future? Quaternary Science Review 29, 1779–1790.

Ortiz, J.D., Orsburn, C., Polyak, L., Grebmeier, J.M., Darby, D.A., Eberl, D.D., Naidu, S., Nof, D., 2009. Provenance of Holocene sediment on the Chukchi Shelf–Alaskan margin based on combined diffuse spectral reflectance and quantitative X-Ray Diffraction analysis. Global and Planetary Change 68, 73–84.

Park, Y.H., Yamamoto, M., Nam, S.-I., Irino, T., Polyak, L., Harada, N., Nagashima, K., Khim, B.-K., Chikita, K., Saitoh, S.-I., 2014. Distribution, source and transportation of glycerol dialkyl glycerol tetraethers in surface sediments from the western Arctic Ocean and the northern Bering Sea. Marine Chemistry.

Patwardhan, A.P., Thompson, D.H., 1999. Efficient synthesis of 40-and 48-membered tetraether macrocyclic bisphosphocholines. Organic letters 1, 241–244.

Pearson, E. J., Juggins, S., Talbot, H. M., Weckström, J., Rosén, P., Ryves, D. B., Roberts, S. J., Schmidt, R., 2011. A lacustrine GDGT-temperature calibration from the Scandinavian Arctic to Antarctic: Renewed potential for the application of GDGT-paleothermometry in lakes. Geochimica et Cosmochimica Acta 75, 6225–6238.

Peterse, F., Meer, J. V. D., Schouten, S., Weijers, J. W.H., Fierer, N., Jackson, R. B., Kim, J.-H., Sinninghe Damsté, J. S., 2012. Revised calibration of the MBT–CBT paleotemperature proxy based on branched tetraether membrane lipids in surface soils. Geochimica et Cosmochimica Acta 96, 215–229.

Pickart, R.S., 2004. Shelfbreak circulation in the Alaskan Beaufort Sea: Mean structure and variability. Journal of Geophysical Research 109, C04024, doi:10.1029/ 2003JC001912.

Pickart, R.S., Weingartner, T.J., Pratt, L.J., Zimmermann, S., Torres, D.J., 2005. Flow of winter-transformed Pacific water into the Western Arctic. Deep Sea Research II 52, 3175–3198.

Biogeosciences Discuss., doi:10.5194/bg-2016-529, 2016
Manuscript under review for journal Biogeosciences
Published: 19 December 2016

Polyak, L., Bischof, J., Ortiz, J., Darby, D., Channell, J., Xuan, C., Kaufman, D., Lovlie, R., Schneider, D., Adler, R., 2009. Late Quaternary stratigraphy and sedimentation patterns in the western Arctic Ocean. Global and Planetary Change 68, 5–17.

Polyak, L., Belt, S.T., Cabedo-Sanz,P., Yamamoto, M., Park, Y.-H., 2016. Holocene sea-ice conditions and circulation at the Chukchi-Alaskan margin, Arctic Ocean, inferred from biomarker proxies. The Holocene, DOI: 10.1177/0959683616645939

Reimer, P. J., Bard, E., Bayliss, A., Beck, J. W., Blackwell, P. G., Ramsey, C. B., Buck, C.E., Cheng, H., Edwards, R.L., Friedrich, M., Grootes, P.M., Guilderson, T.P., Haflidason, H., Hajdas, I., Hatté, C., Heaton, T.J., Hoffmann, D.L., Hogg, A.G., Hughen, K.A., Kaiser, K.F., Kromer, B., Manning, S.W., Niu, M., Reimer, R.W., Richards, D.A., Scott, E.M., Southon, J.R., Richard, A.S., Turney, C.S.M., van der Plicht, J., 2013. IntCal13 and Marine13 radiocarbon age calibration curves, 0–50,000 years cal BP.

Schouten, S., Hopmans, E.C., Schefuß, E., Sinninghe Damsté, J.S., 2002. Distributional variations in marine crenarchaeotal membrane lipids: a new tool for reconstructing ancient sea water temperatures? Earth and Planetary Science Letters 204, 265–274.

Schouten, S., Huguet, C., Hopmans, E.C., Kienhuis, M.V.M., Sinninghe Damsté, J.S., 2007. Analytical methodology for TEX_{86} paleothermometry by high performance liquid chromatography/atmospheric pressure chemical ionization-mass spectrometry. Analytical Chemistry 79, 2940–2944.

Screen, J.A., Simmonds, I., 2010. The central role of diminishing sea ice in recent Arctic temperature amplification. Nature 464, 1334–1337.

Shimada, K., Carmack, E., Hatakeyama, K., and Takizawa, T., 2001. Varieties of shallow temperature maximum waters in the Western Canadian Basin of the Arctic Ocean:

Biogeosciences Discuss., doi:10.5194/bg-2016-529, 2016
Manuscript under review for journal Biogeosciences
Published: 19 December 2016

Geophysical Research Letters 28, 3441–3444.

Shimada, K., Kamoshida, T., Itoh, M., Nishino, S., Carmack, E., McLaughlin, F., Zimmermann, S., Proshutinsky, A., 2006. Pacific Ocean inflow: Influence on catastrophic reduction of sea ice cover in the Arctic Ocean. Geophysical Research Letters 33, L08605, doi:10.1029/2005GL025624.

Sinninghe Damsté, J.S., Hopmans, E.C., Pancost, R.D., Schouten, S., Geenevasen, J.A.J., 2000. Newly discovered non-isoprenoid dialkyl diglycerol tetraether lipids in sediments. Chemical Communications 23, 1683–1684.

Tierney, J. E., Russell, J. M., Eggermont, H., Hopmans, E. C., Verschuren, D., Damsté, J. S., 2010. Environmental controls on branched tetraether lipid distributions in tropical East African lake sediments. Geochimica et Cosmochimica Acta 74, 4902–4918.

Viscosi-Shirley, C., Pisias, N., Mammone, K., 2003. Sediment source strength, transport pathways and accumulation patterns on the Siberian–Arctic's Chukchi and Laptev shelves. Continental Shelf Research 23, 1201–1225.

Weijers, J.W.H., Schouten, S., van Den Donker, J.C., Hopmans, E.C., Sinninghe Damsté, J.S., 2007. Environmental controls on bacterial tetraether membrane lipid distribution in soils. Geochimica et Cosmochimica Acta 71, 703–713.

Weingartner, T., Aagaard, K., Woodgate, R., Danielson, S., Sasaki, Y., Cavalieri, D., 2005. Circulation on the north central Chukchi Sea shelf. Deep-Sea Research II 52, 3150–3174.

Williams, W.J., Melling, H., Carmack, E.C., Ingram, R.G., 2008. Kugmallit Valley as a conduit for cross–shelf exchange on the Mackenzie Shelf in the Beaufort Sea. Journal of Geophysical research 113, C02007, doi:10.1029/2006JC003591.

Woodgate, R.A., Aagaard, K., 2005. Revising the Bering Strait freshwater flux into the Arctic Ocean. Geophysical Research Letters 32, L02602, doi:10.1029/2004GL021747.

Woodgate, R.A., Aagaard, K., Swift, J.H., Falkner, K.K., Smethie, W.M., 2005a. Pacific Ventilation of the Arctic Ocean's lower halocline by upwelling and diapycnal mixing over the continental margin. Geophysical Research Letters 32, L18609, doi:10.1029/2005GL023999.

Woodgate, R.A., Aagaard, K., Weingartner, T., 2005b. A Year in the physical oceanography of the Chukchi Sea: Moored measurements from autumn 1990–1991. Deep-Sea Research II 52, 3116–3149.

Yamamoto, M., Okino, T., Sugisaki, S., Sakamoto, T., 2008. Late Pleistocene changes in terrestrial biomarkers in sediments from the central Arctic Ocean. Organic Geochemistry 39, 754–763

Yamamoto, M., Polyak, L., 2009. Changes in terrestrial organic matter input to the Mendeleev Ridge, western Arctic Ocean, during the Late Quaternary. Global and Planetary Change 68, 30–37.

Yunker, M.B., Macdonald, R.W., Cretney, W.J., Fowler, B.R., McLaughlin, F.A., 1993. Alkane, terpene, and polycyclic aromatic hydrocarbon geochemistry of the Mackenzie River and Mackenzie shelf: Riverine contributions to Beaufort Sea coastal sediment. Geochimica et Cosmochimica Acta 57, 3041–3061.

Yunker, M.B., Macdonald, R.W., Snowdon, L.R., Fowler, B.R., 2011. Alkane and PAH biomarkers as tracers of terrigenous organic carbon in Arctic Ocean sediments, Organic Geochemistry 42, 1109–1146.

Yurco, L.N., Ortiz, J.D., Polyak, L., Darby, D.A., Crawford, K.A., 2010. Clay mineral cycles identified by diffuse spectral reflectance in Quaternary sediments from the Northwind Ridge: implications for glacial–interglacial sedimentation patterns in the Arctic Ocean. Polar Research 29, 176–197.

Zhang, Y.G., Zhang, C., Liu, X.-I., Li, L., Hinrichs, K.U., Noakes, J.E., 2011. Methane index: A tetraether archaeal lipid biomarker indicator for detecting the instability of marine gas hydrates. Earth and Planetary Science Letters 307, 525–534.

Biogeosciences Discuss., doi:10.5194/bg-2016-529, 2016
Manuscript under review for journal Biogeosciences
Published: 19 December 2016

576 Table 1. Information of sediment cores used in this study

Cruise name	Core name	Latitude (ºN)	Longitude (ºW)	Water depth (m)	Core length (cm)
ARA02B	01A-GC	73.63	166.52	119	563
HLY0501	05TC/JPC	72.70	157.45	462	1648
HLY0501	06JPC	72.69	157.03	673	1554
HLY0501	08TC/JPC	71.63	156.84	90	1396

577

Figure captions

Fig. 1. Index map with location of sediment cores under study and a generalized bathymetry. Arrows indicate major currents in the Chukchi Sea: Siberian Costal Current (brown color) and three branches of Pacific water flowing through the Bering Strait (orange color). The blue-sky and red dashed lines indicate summer sea-ice margin (15% concentration) for the late 20th century average and the all-time observational 2012 minimum, respectively (data from the National Snow and Ice Data Center).

Fig. 2. GDGT distribution in surface sediments of the Chukchi Sea and adjacent western Arctic Ocean and northern Bering Sea: concentrations of (A) isoprenoid GDGTs and (B) branched GDGTs, (C) BIT indices, (D) TEX_{86}^{L}, (E) TEX_{86}, (F) CBT and (G) MBT' indices (Park et al., 2014).

Fig. 3. Age-depth distribution of calibrated ^{14}C ages in cores under study

Fig. 4. The average fractional abundance of isoprenoid and branched GDGTs, respectively, in (a) surface sediments from the Chukchi Sea and the adjacent western Arctic Ocean and northern Bering Sea (Park et al., 2014) grouped by geographic environment type, and (b-d) cores in this study. The core data is shown in major stratigraphic intervals: late, middle, and early Holocene, deglacial, and pre-LGM.

Fig. 5. Downcore plots of linear sedimentation rates (LSR) and distribution of GDGT (this study) and IP_{25} (Polyak et al., 2016). Dashed lines indicate the lower boundary of the full

Biogeosciences Discuss., doi:10.5194/bg-2016-529, 2016
Manuscript under review for journal Biogeosciences
Published: 19 December 2016

marine sedimentary unit around ca. 9 ka, with some variance probably due to imperfect age control. Note a break in the age scale between 05JPC and 06JPC samples.

Fig. 6. MBT' vs. CBT plots. Values above the dotted line correspond to surface-sediment data from Arctic rivers and from perennially sea-ice covered Arctic Ocean (Park et al., 2014). Data points are color-coded by major paleoenvironmental intervals identified in cores under study (approximate ages with some variance due to imperfect age control).

Biogeosciences Discuss., doi:10.5194/bg-2016-529, 2016
Manuscript under review for journal Biogeosciences
Published: 19 December 2016

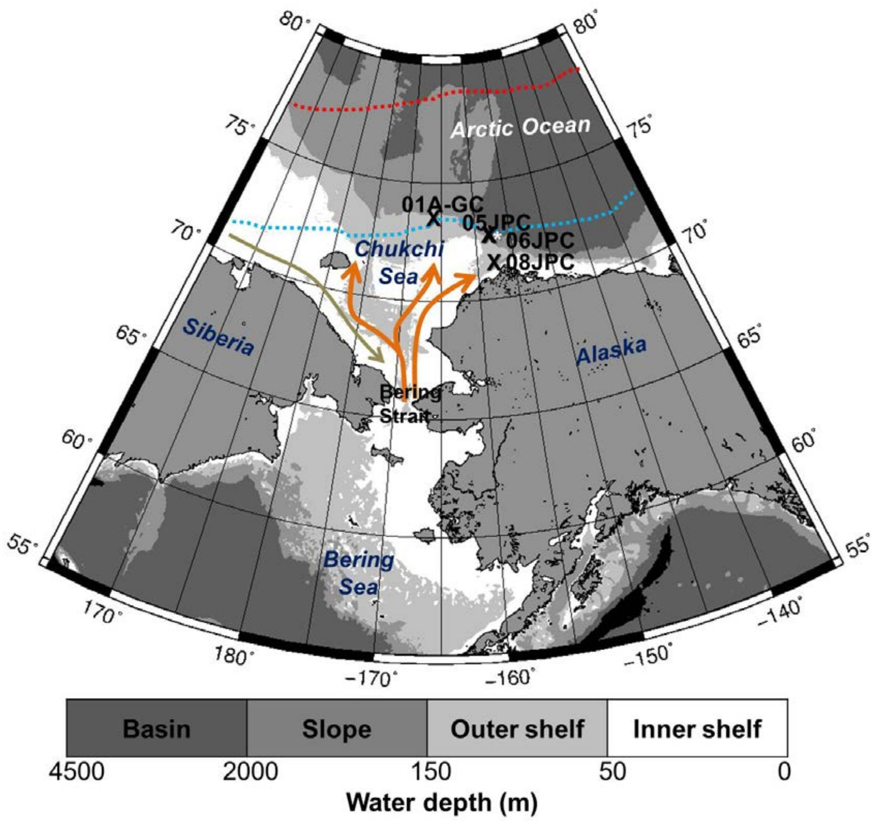

Fig. 1.

Biogeosciences Discuss., doi:10.5194/bg-2016-529, 2016
Manuscript under review for journal Biogeosciences
Published: 19 December 2016

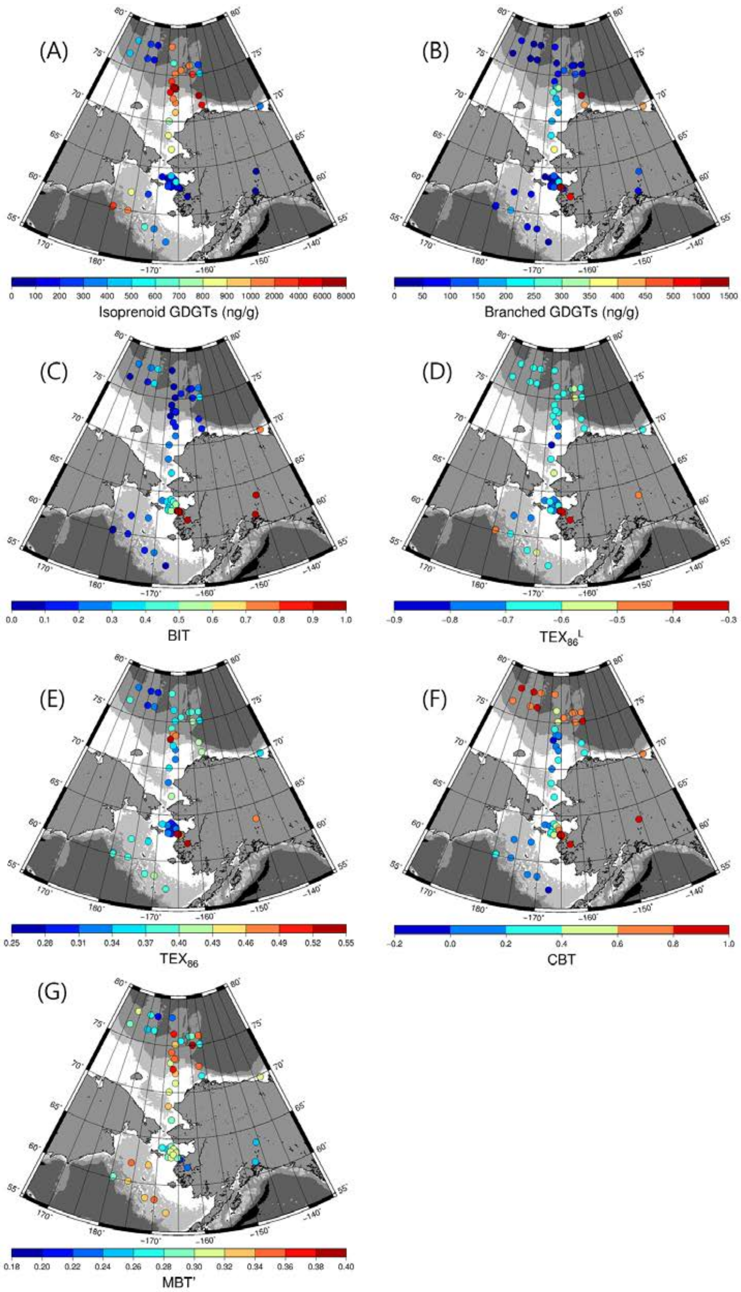

612

613 Fig. 2.

614

Biogeosciences Discuss., doi:10.5194/bg-2016-529, 2016
Manuscript under review for journal Biogeosciences
Published: 19 December 2016

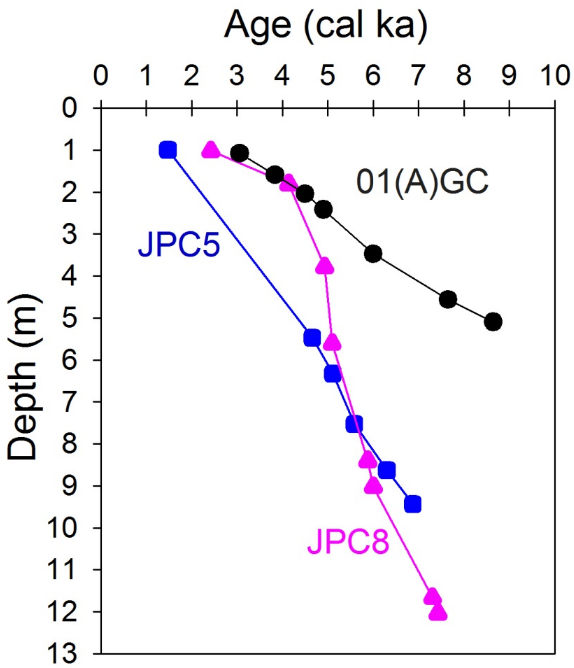

615

616 Fig. 3.

617

Biogeosciences Discuss., doi:10.5194/bg-2016-529, 2016
Manuscript under review for journal Biogeosciences
Published: 19 December 2016

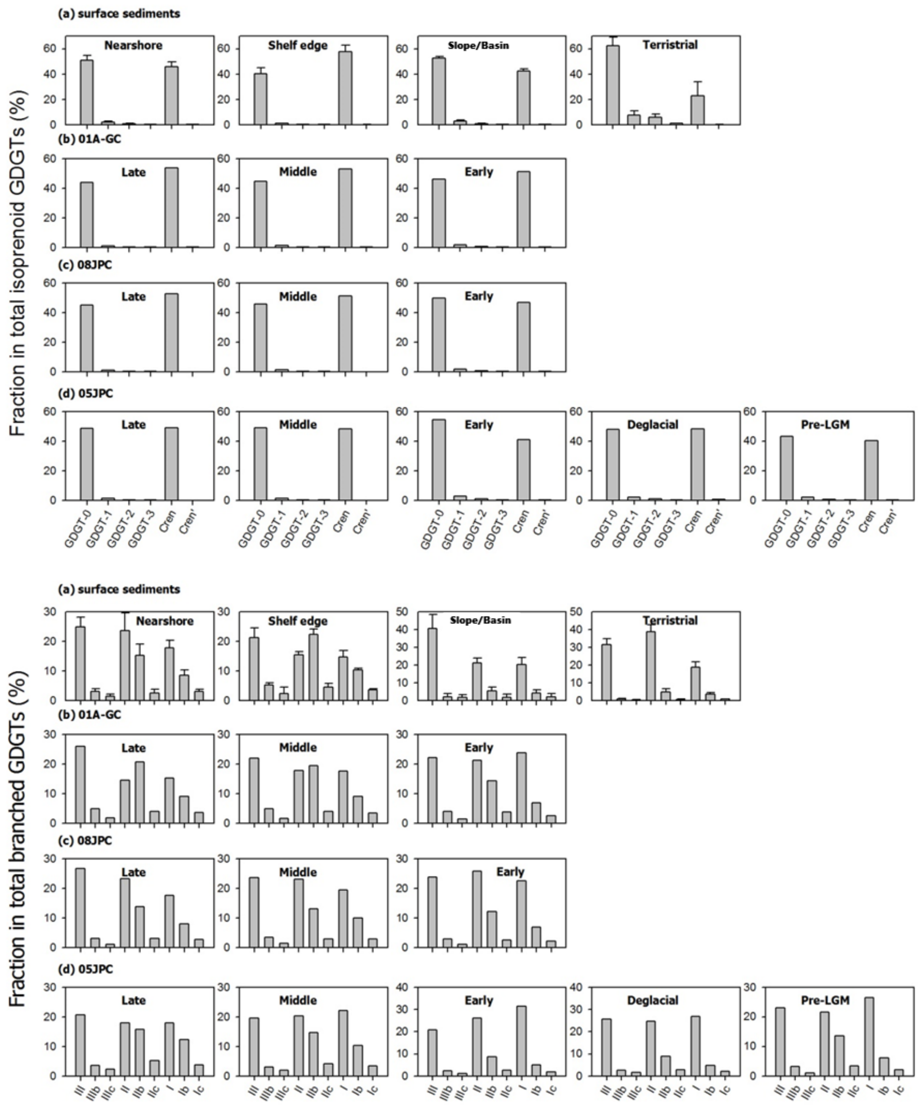

Fig. 4.

Biogeosciences Discuss., doi:10.5194/bg-2016-529, 2016
Manuscript under review for journal Biogeosciences
Published: 19 December 2016

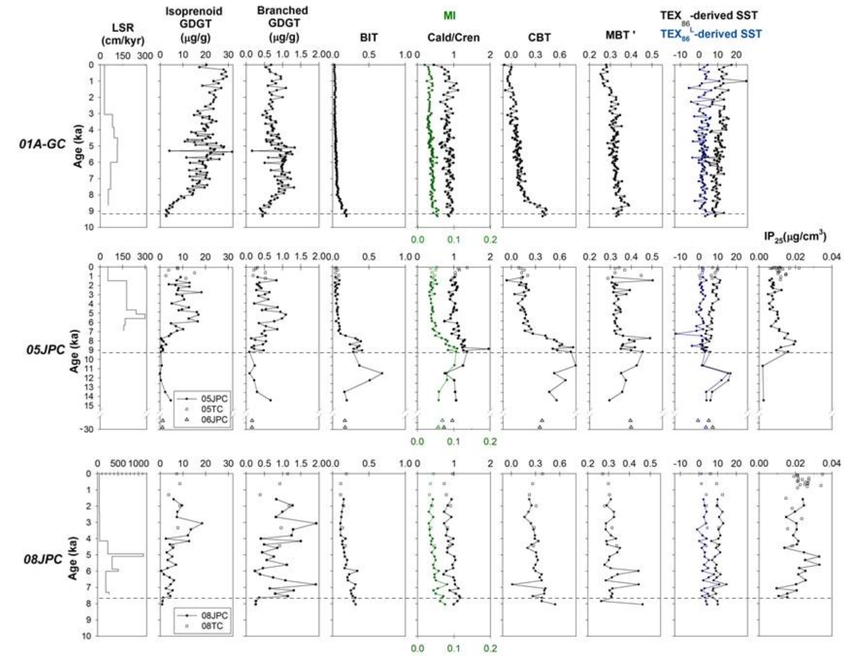

Fig. 5.

Biogeosciences Discuss., doi:10.5194/bg-2016-529, 2016
Manuscript under review for journal Biogeosciences
Published: 19 December 2016

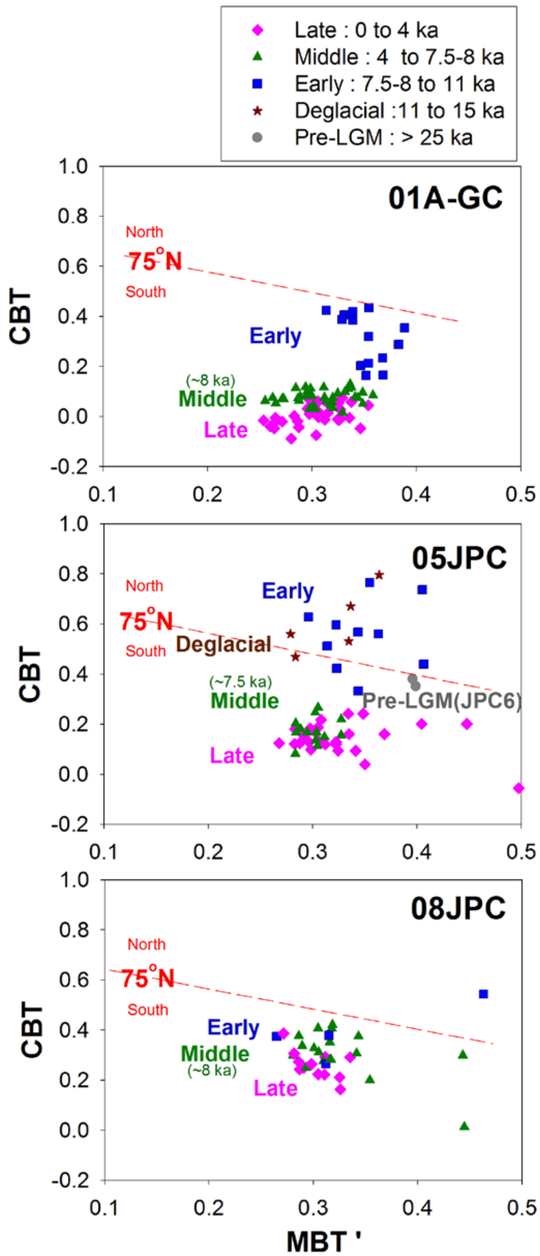

623

624 Fig. 6.

Biogeosciences Discuss., doi:10.5194/bg-2016-529, 2016
Manuscript under review for journal Biogeosciences
Published: 19 December 2016

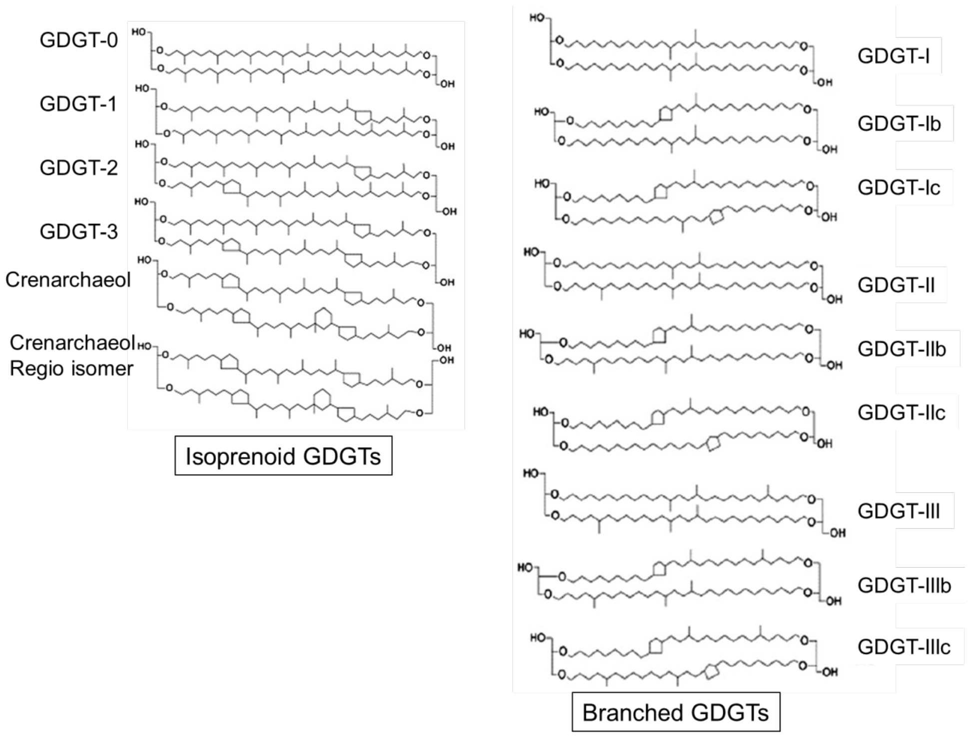

Appendix